

Blowoff propensity, CRZs and Flow Turbulent structure using a range of Syngas compositions for Gas Turbines
Hesham Baej^{a*}, Agustin Valera-Medina^a, Nick Syred^a, Richard Marsh^a, Phil Bowen^a

^a College of Physical Sciences and Engineering, Cardiff University, CF24 3AA

* Corresponding author. Email: baejh@cardiff.ac.uk; Tel. +44 (0)2920 875948

Abstract

This paper presents a series of experiments and numerical simulations using commercial software (ANSYS) to determine the behaviour and impact on the blowoff process with various geometries and simulated syngas compositions at fixed power outputs. Experiments were performed using a generic premixed swirl burner. The Central Recirculation Zone and the associated turbulent structure contained within it were obtained through CFD analyses providing details of the structures and the Damkohler Number (Da) close to blowoff limits. The results show how the strength and size of the recirculation zone are highly influenced by the blend, with a shift of Da and turbulence based on carbon-hydrogen ratio, shearing flows and Reynolds number.

Instabilities such as thermoacoustics, flashback, autoignition and blowoff are highly affected by the flow structures and chemical reactions/diffusivity. Moreover, it has been observed that turbulence close to the boundaries of the central recirculation zone, a region of high stability for swirling flows, is highly altered by the chemical characteristics of the fuel blends. In terms of blowoff, the phenomenon is still not entirely understood. As the process occurs, its theoretical limits do not match its real behaviour. Therefore, one possibility could be the difference in turbulence and Da numbers across the flame, being critical at the base of the flame where the system is stabilized.

Nomenclature

S	Swirl number [-]	G	Stretch factor [-]
CRZ	Central Recirculation Zone	erfc	Complementary error function
Da	Damkohler number [-]	σ	standard deviation of the distribution of ϵ
τ	Turbulent time scale [s]	gcr	Critical rate of strain[-]
τ_c	Chemical time scale [s]	μ_{str}	stretch factor coefficient for dissipation pulsation
α	Thermal diffusivity M2/s	L	Turbulent integral length
U _i	Laminar flame speed [m/s]	η	Kolmogorov micro-scale

1 Introduction

Premixed flame stabilization in high intensity combustion is an important topic of study for the high efficiency and low emission operation of gas turbine combustors and industrial furnaces. Current lean premixing combustion technologies (LPM) focus on operation at very low equivalence ratios in order to reduce thermal NO_x production. However, gas turbine operation with a potentially range of fuels presents a problem in terms of variation of heating values, flame speeds and Wobbe Index. Process and refinery gases and gasified coal or petcoke are just a few examples. The biggest challenge to fuel-flexibility of most combustors is the large differences between natural gas and the proposed replacement fuels. Moreover, gas turbines must meet the current emissions regulations, which often mean running at ultra-lean conditions near the blowoff limit. However, blowoff continues to be a phenomenon that is difficult to predict across reactor types and fuel compositions. To describe the lean blowoff behaviour of such burners under various fuel compositions, correlations have to be determined and simplified models developed to further the implementation of fuel flexible technologies [1]. Most current gas turbines use swirl stabilized combustion, as it creates a flow field that anchors the flame and stabilizes the combustion process [2]. The crucial feature of swirl burners is the formation of a central recirculation zone (CRZ) which extends blowoff limits by recycling heat

and active chemical species to the root of the flame in the burner exit [3-4]. Thus, the CRZ is one of the mechanisms for flame stabilization that through an aerodynamically decelerated region creates a point where the local flame speed and flow velocity match [5].

A significant amount of literature exists on measuring, correlating and predicting blowoff limits for bluff body and swirl stabilized combustors. There are three basic characterizations of the physical phenomena responsible for blowoff. Longwell et al [6] suggested that blowoff occurs when it is not possible to balance the rate of entrainment of reactants into the recirculation zone, viewed as a well stirred reactor, and the subsequent turbulent burning velocity of the mixture. Since entrainment rates scale as the size of the CRZ increases and velocity of the flow is decreased, then it follows that this criterion reduces to a Damkohler number (Da) blowoff criterion, using a chemical time that is derived from the well stirred reactor theory [6]. The Damkohler number used in turbulent combustion, corresponds to the ratio of chemical time scale τ_c and turbulent time scale τ_t , can be expressed as,

$$Da = \tau_t / \tau_c \quad (1)$$

$$\tau_c = \alpha / U_i^2 \quad (2)$$

As an example, most practical swirl combustion reactions take place at the lower limit, i.e. where $Da \ll 1$, so the turbulence timescales are significantly shorter than the chemistry.

With some caveats noted by Shanbhogue et al. [7], there is general agreement that the blowoff process is controlled by a competition between the fluid mechanical and chemical kinetic processes, which can subsequently be defined in terms of a Damköhler number. Therefore blowoff occurs when the heat required by the combustible stream exceeds that received from the recirculation zone. A different view is that the contact time between the combustible mixture and hot gases in the shear layer must exceed a certain chemical ignition time. This implies a direct link between the scale of the characteristic dimension of the recirculation zone length, leading to a similar Da criterion [7]. Current theories are based on a flamelet based description upon local extinction by excessive flame stretch [8]. Flame stretching starts blowoff with the initiation of holes in the flame that are filled by the same flame creating stretching in areas that otherwise would have been unaffected. The flame will extinguish when the stretch rate exceeds a critical value [7].

Turbulence is also an important parameter in blowoff limits. Research by Peters [9] resulted in a theory of turbulent premixed flames that becomes generally accepted in the combustion research community. Experimental observations (e.g. Schlieren photography, laser sheet imaging techniques, etc.) have revealed that, in general, the structure of a turbulent premixed flame is to be seen as superimposed instantaneous contours of convoluted reaction zones. The appearance of the reaction zone depends heavily on the governing turbulent structures and the chemical properties of the flow. Thus, fuel compositions produced from a potentially variable composition syngas will result in a multitude of chemical properties in terms of thermal diffusivity, density, laminar flame speed, and heating value. The experiments conducted by Lieuwen et al [10] to investigate the impact of fuel composition on the operability of lean premixed gas turbine combustors have focused on H₂/CH₄ flames and show that small additions of H₂ substantially enhance the mixture's resistance to extinction or blowoff. Fundamental studies show that the extinction strain rate of methane flames is doubled with the addition of 10% H₂. Similarly, CO/CH₄ flames showed a variance in their extinction strain rate. Experiments were also conducted using N₂, H₂O and CO₂. They concluded that the flame speeds of mixtures with CO₂ dilution are lower than those of mixtures diluted with chemically inert species with the same specific heat as CO₂. CO₂ dilution can lead to lower laminar flame speeds and lower flame temperatures due to radiative losses from the flame, which can also impact subsequent emissions [10]. Correlations of the turbulent flame speed was obtained in the form of $S_T = S_L \cdot f(u')$. They showed that as the turbulence intensity increases, the turbulent flame speed initially increases. The main factor influencing changes in turbulent flame speed due to varying fuel composition is via the laminar flame speed. However, turbulence intensity and laminar flame speed alone do not capture many important characteristics of the turbulent flame speed. One must also consider the effects of flame instabilities and flame stretch [10].

Lee et al [11] investigated the combustion performance of syngas comprised of hydrogen, carbon monoxide, nitrogen, carbon dioxide and steam, evaluating the dilution effect of the inert fractions. It was observed that NOx decreased as the amount of diluents is increased. They report that nitrogen, carbon dioxide and/or steam are applicable to a syngas turbine to control NOx emission while ensuring reliable operation, thus the blowoff limit could be influence by control of these gases [11]. Strakey et al [12] studied the effects of hydrogen addition on flame extinction in a lean-premixed swirl-stabilized combustor operating on natural gas and air. Hydrogen concentration in the fuel was changed from 0 to 80% by mass. They observed that increasing the hydrogen concentration in the fuel reduced the equivalence ratio before blowoff from 0.46 to 0.30. Schefer et al [13] conducted experiments on combustion characteristics of a premixed, swirl-stabilized flame to determine the effects of enriching methane with hydrogen under fuel-lean conditions. Hydrogen addition resulted in a significant change in the flame structure, indicated by a shorter and more robust flame [13].

In Computational Fluid Dynamics (CFD), the flame stretch concept could be applied to understand physical processes related to laminar flame studies in the area of flame stabilization, laminar flame speed determination and flammability limits [14]. Premixed combustion is more difficult to simulate than non-premixed combustion. Therefore, the flame propagation can be modelled by solving transport equations of the weighted mean density reaction progress variable denoted by c based on the Zimont model [14]. In this model, the stretch factor (G) represents the likelihood that the stretching will not quench the flame, i.e. if there is no stretching ($G=1$), the probability that the flame will be unquenched is 100%. The stretch factor is obtained by integrating the log-normal distribution of turbulence dissipation rate, ϵ :

$$G = 1/2 \operatorname{erfc} \{-\sqrt{1/2\sigma} [\operatorname{Ln}(\epsilon_{cr}/\epsilon)] + \sigma/2\} \quad (3)$$

Considering the flame stretching effects, the critical rate of strain (g_{cr}) should be adjusted based on experimental data. For the numerical models an appropriate value can be determined as [15-16],

$$g_{cr} = BU_i^2/\alpha \quad (4)$$

ϵ_{cr} , the turbulence dissipation rate at the critical rate of strain, is given by,

$$\epsilon_{cr} = 15\nu g_{cr}^2 \quad (5)$$

In this paper the structure of premixed swirl stabilized flames is analysed with the help of various numerical studies and experimental data, correlating the blowoff phenomenon with various syngas compositions in order to classify the flame in a combustion regime. It has been observed that turbulence close to the boundaries of the central recirculation zone is impacted by outlet geometries and chemical properties of the fuel mixture. The aim of this paper is to correlate measurements of the turbulence across the flame and the central recirculation zone by comparison of the turbulence of the boundaries of the region and the Da number which will give a good indication of the differences between the reaction and diffusivity rates of all the specific blends.

2 Setup

A generic swirl burner constructed from stainless steel was used to examine the flame stability limits at atmospheric conditions (1bar, 293K) at Cardiff University's Gas Turbine Research Centre (GTRC). A photograph and schematic of the generic burner is presented in Figure 1. More details can be found in previous literature [19]. A geometrical Swirl number, S_g , of 1.05 was used. The recirculation zone was distorted using a 30°, 45° and 60° nozzles, shown in Figure 2, as observed by Valera-Medina et al [4]. Confined and unconfined conditions were tested. Confinement was done using a quartz cylinder with a diameter of 3D, being D the external nozzle diameter of 0.028m.



Figure 1: Unconfined swirl burner and schematic diagram.

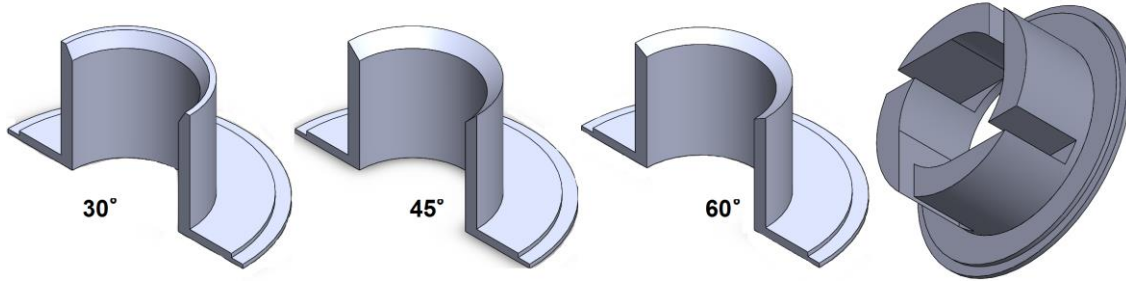


Figure 2: Angular nozzle and geometrical swirl respectively.

Experiments were conducted to define the blowoff limits and swirling frequency shift of different configurations using different gases under confined conditions. The gases used were a mixture of CH_4 , CO , and are specified in Table 1.

Table 1: Syngas compositions

Gas number	Gas compositions
Syngas 1	10% CH_4 + 45% H_2 + 45% CO
Syngas 2	20% CH_4 + 40% H_2 + 40% CO
Syngas 3	30% CH_4 + 35% H_2 + 35% CO
Syngas 4	50% CH_4 + 25% H_2 + 25% CO
Gas 5	100% CH_4
Gas 6	50% CH_4 + 50% CO_2

Table 2. Experimental and all CFD conditions examined

Gas Number	\dot{M}_{fuel} [g/s]	\dot{M}_{Air} [g/s]	Nozzle angle	Total [g/s]	Φ	Power Output KW
Syn1	0.101	1.414	30°	1.515	0.425	7.489
Syn1	0.101	1.405	45°	1.507	0.428	7.489
Syn1	0.101	1.383	60°	1.485	0.453	7.489
Syn2	0.104	1.557	30°	1.661	0.485	7.489
Syn2	0.104	1.554	45°	1.658	0.486	7.489
Syn2	0.104	1.489	60°	1.593	0.508	7.489
Syn3	0.107	1.631	30°	1.738	0.563	7.489
Syn3	0.107	1.677	45°	1.784	0.548	7.489
Syn3	0.107	1.650	60°	1.757	0.557	7.489
Syn4	0.113	1.839	30°	1.953	0.689	7.489
Syn4	0.113	1.791	45°	1.905	0.707	7.489
Syn4	0.113	1.832	60°	1.9461	0.692	7.489

Numerical Methodology

Isothermal conditions with no combustion were used to calibrate the system and indicate the size of the central recirculation zone (CRZ), although it is well known that there are also 3D time dependant coherent structures present and thus the results are of an indicative nature. During the simulation,

various types of solvers were investigated and conclusions drawn as to which were the most effective. Based on the experimental results obtained at 1.485 g/s to 1.946 g/s the best option for the present work was the κ - ω SST model [14, 17-18].

$$\partial\rho/\partial t + \text{div}(\rho U) = 0 \quad (6)$$

$$\rho D_{ui}/D_t = -\partial p/\partial x_i + \text{div}(\mu \text{grad } u_i) + S_{Mi} \quad (7)$$

$$\begin{aligned} \rho DE/Dt = & \text{div}(\rho U) + [\partial(u\tau_{xx})/\partial x + \partial(u\tau_{yx})/\partial y + \partial(u\tau_{zx})/\partial z + \partial(v\tau_{xy})/\partial x + \partial(v\tau_{yy})/\partial y + \\ & (\partial(v\tau_{zy})/\partial z + \partial(w\tau_{xz})/\partial x + \partial(w\tau_{yz})/\partial y + \partial(w\tau_{zz}) \\ & / \partial y] + \text{div}(k \nabla T) + S_E \end{aligned} \quad (8)$$

Simulations were performed using all syngases in Table 1 under premixed conditions with FLUENT 14.5. The pre-processors used to construct the model grid were the FLUENT in-built package and ICEM 14.5.7. After independency mesh analyses, it was concluded that a medium size mesh of ~796,878 nodes and 796,878 elements would provide similar results with both pre-processors. A finer mesh was created close to the burner exit and around the fuel nozzles, visible in Figure 4. All the CFD analyses were conducted using an output power of 7.49 kW. Non-slip boundary conditions were defined using adiabatic conditions at 1 bar pressure and inlet temperatures of 300K.

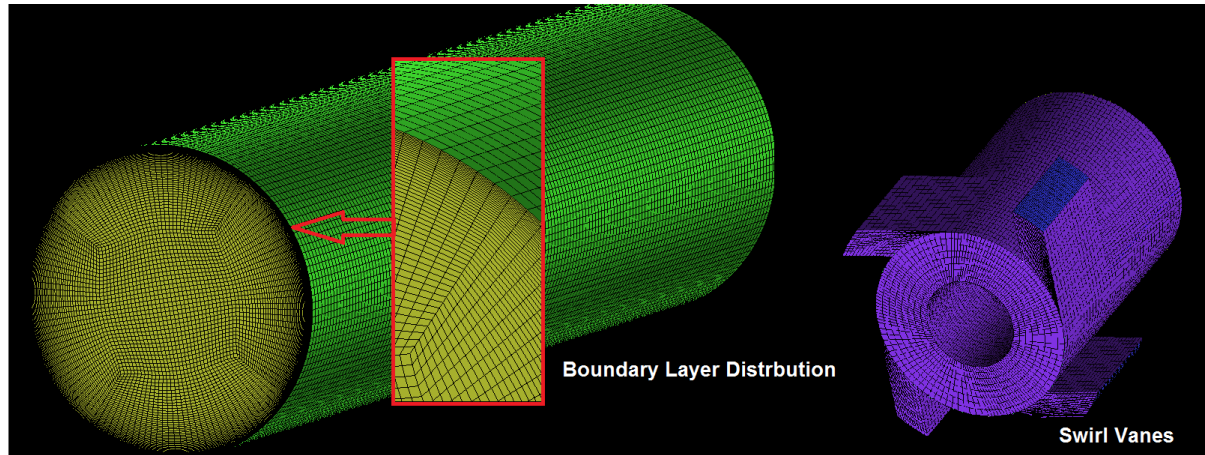


Figure 4: Mesh Distribution and boundary layer

Results & Discussions

Experiments

Figure 5 shows the comparison between the 3 nozzles. For a comparable operating condition be achieved, equivalence ratio reductions of ~20% were observed with all nozzles when using confinement, hence it can be said that the burner operated at leaner conditions with the confinement. Figures 5 and 6 illustrate the operating equivalence ratios with the syngas compositions tested. As the mole fraction of hydrogen increases the equivalence ratio at which LBO occurs moves to leaner conditions, thus showing an improvement in blowoff limits. It can be seen that some trends follow linear progressions, especially during the experiments using the 45° nozzle and syngas-1. As the angle is decreased/increased, the results become less linear, implying a breakdown in the controlling phenomena due to a more chaotic process.

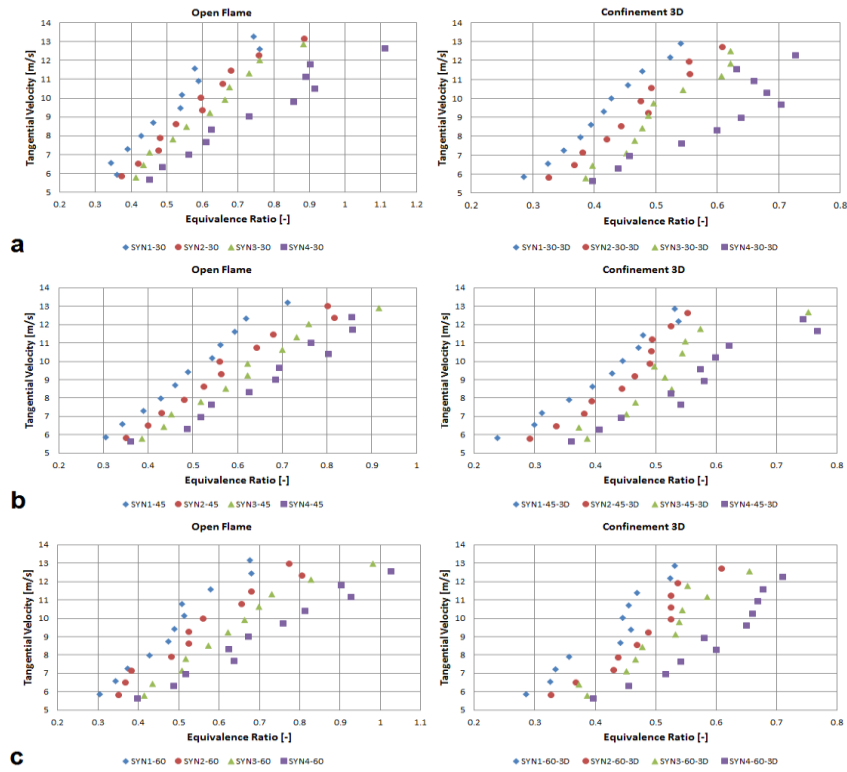


Figure 5: Comparison of blowoff limits, with different nozzle geometries a, b and c.

Similarly, the decrease in hydrogen produces less homogeneous results. This relates to the high reaction of hydrogen close to the dumping plane. The increase of H_2 decreases the Da number as a consequence of faster chemical reactions. Thus, convective processes and turbulence produced by the CRZ and shearing flows do not appear to be controlling the onset of LBO. However, the reduction of hydrogen produces conditions where the presence of these structures creates a less linear, more random behaviour towards the blowoff limit.

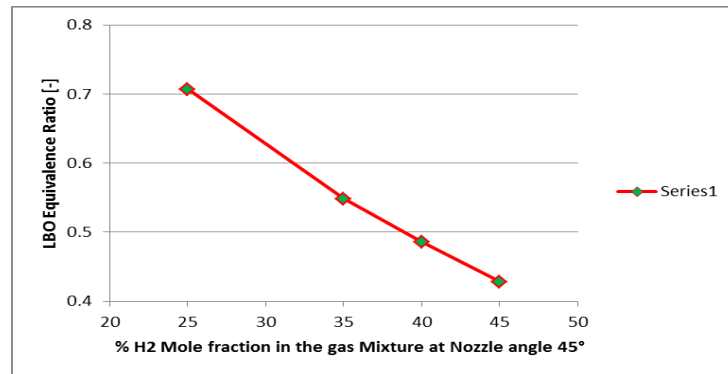


Figure 6. Effect of the H_2 content on the LBO equivalence ratio

A comparison of blowoff limits, Figure 7, demonstrates the effects of the different fuels, plus data taken with pure methane and methane blended with carbon dioxide using a 45° nozzle [19]. There is a considerable improvement in LBO with the increase of hydrogen. Also, syngas 4 with a 50% methane shows the same LBO values that pure methane. This demonstrates that although Da values are different between the two gases, blowoff occurs at the same equivalence ratios as a consequence of mechanisms that might be produced by coherent structures that produce greater effects on blowoff at these lower reaction time scales.

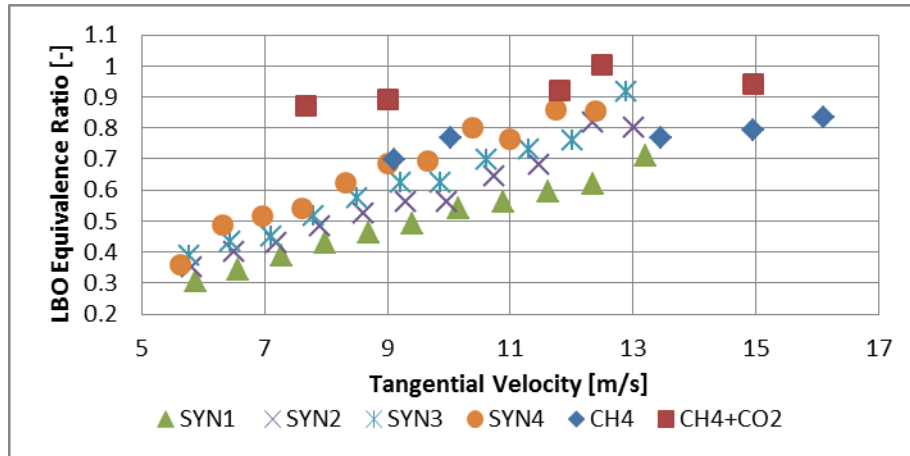


Figure 7: LBO equivalence ratios of different fuel mixtures at same swirl numbers and nozzle 45°.

The blowoff process was observed to start with the reduction of the flame to a point of annihilation. Once reaching this point, the flame would start oscillating in a transverse direction, with the re-ignition of the blend at low frequencies as a consequence of the recirculation of gases. The stronger CRZ observed under isothermal conditions [4] pulls back some of the hot products that will find a point of high interaction with the reactants between the CRZ and the outgoing flow. It was believed this region could be the place where the CRZ and the Precessing Vortex Core interact, a region that shows the highest turbulence in the flow [4]. Since this interaction will depend on the strength and shape of the CRZ-PVC structure, therefore, it was expected a greater dependency on geometry. However, at low flow rates just a slight dependency was observed, Figure 8a. Hydrogen content variation, thus the resulting change in Da , was more important to the phenomenon. This is believed to be caused by the weaker CRZ-PVC interaction at these low Re . Moreover, being a localized phenomenon, the weaker CRZ-PVC interaction will allow the re-establishment of the flame in other regions. Thus, it is believed that the hydrodynamic interaction between the CRZ-PVC plays a minor role in the blowoff for these hydrogen enriched blends at these conditions. The influence of the nozzle shows a slight effect for all cases at low and medium flowrates. However with syngas 4, as Re was increased, there was a considerable shift in equivalence ratios using all nozzles as a consequence of the reduction of H_2 and distortion of the CRZ, thus CRZ-PVC interaction is believed to be a critical part of the blowoff process at high flow rates and lower chemical reaction times, Figure 8b.

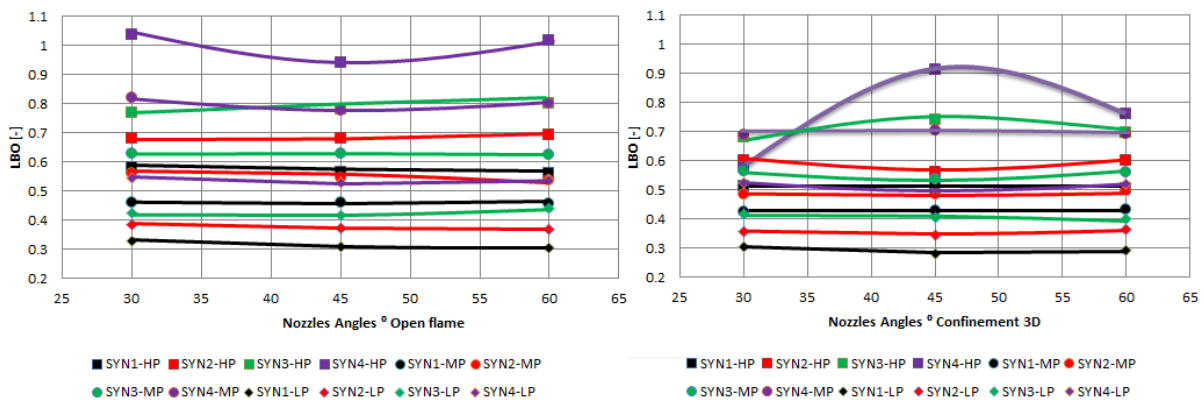


Figure 8 : Comparison of the effect of outlet nozzle angle on LBO equivalence ratio for all syngases at a) low flow rate 1.233g/s and b) high flow rates 2.294g/s.

Final blowoff was produced after a longer flame appeared with an intermediate constriction at the centre, Figure 9. The flame showed a cycle of ignition, elongation and quenching just before increasing the flowrate for the final annihilation of the flame. The observed constriction seems to be formed by the reaction of the reactants around the CRZ and a secondary recirculation zone that forms further downstream from the burner mouth. It is believed that this second recirculation, previously

observed in other works [4] is defined by the baroclinic depression in the central region caused by the swirling motion, the strength of the main CRZ and acoustics of a 3/4 wave. More research is required on this point.



Figure 9: Pulsating flame. Progression of LBO seconds before final onset. $S = 1.05$, $\Phi = 0.525$. Frequency 10Hz.

Numerical results

Different CRZ boundary contours, Figure 10, turbulence studies, Da number, stretch factor and turbulent flame speed, Figure 11, for syngases 1, 2, 3 and 4 using 45° nozzle at 7.49kW were produced as a consequence of the different reactions and localized combustion swirl changes. The velocities and momentum of the flow increase on localised regions of the burner through the High Momentum Flow Region (HMFR) [21]. The point at which the flow becomes negative diverged from $r/D = -0.5$ to 0.5 indicating that the CRZ is increasing its width whilst the HMFR is getting slimmer and stronger as a consequence of the greater negativity of the recirculation structure and squeeze of the shearing flow, Figure 11a. Regarding the CRZ the use of different configurations and fuels has demonstrated that the shape and strength of the structure can change drastically depending on these alterations, Figure 10 and Table 4. Comparing the CRZ size, CFD calculations indicate that the use of the 60° nozzle produces the largest structures, as expected.

The turbulent flame speed and stretch factors, Figure 11b and 11c, show different trends depending on the syngas used, with the increase of hydrogen showing an increase in turbulent flame speed and stretch. The Damkohler number increases along the plenum, Figure 11d, due to the decrease in the turbulent intensity and increase of length scales of the flame as observed in Figure 11b. It is in the boundaries of the CRZ where the length scales go to a minimum, thus increasing turbulent intensity and decreasing Da, which is evident in Figure 11b and 11c. The increase/decrease of chemical reaction time will affect Da and flame stretch as observed in Figure 11c and 11d.

Table 4. Comparison of the CRZ size of four of syngas using three different angular nozzles

Gas	30°		45°		60°	
No	Width	Length	Width	Length	Width	Length
Syn1	1.85D	4.7D	1.9D	4.3D	1.4D	9.6D
Syn2	1.8D	5.2D	1.85D	4.6D	1.8D	4.7D
Syn3	1.9D	5.4D	1.9D	7.2D	1.8D	5.2D
Syn4	1.9D	5.8D	1.9D	4.6D	1.7D	4D

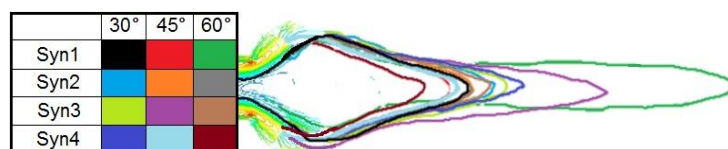


Figure 10: CRZ contours using different syngases.

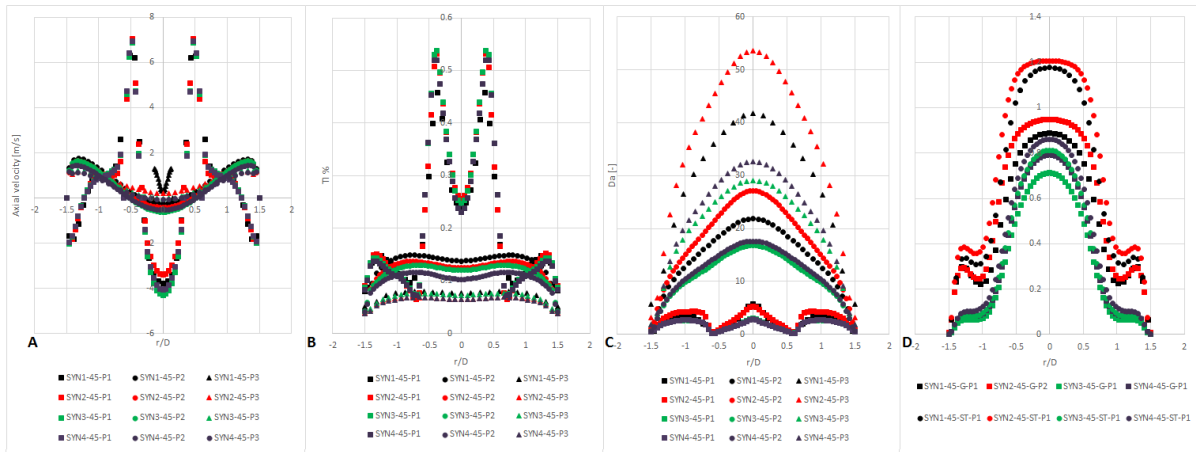


Figure 11: Comparison of (a) axial velocity; (b) turbulent intensity; (c) Damkohler number; (d) Stretch factor and turbulent flame speed across the flame for all syngases using nozzle 45° at 4 different planes P1, P2, P3 and P4 at $X/D = 0.00, 3.57, 7.14$ and 10.7 , respectively.

Conclusion

Experimental tests and numerical simulations have been conducted in an atmospheric, premixed swirl burner to investigate the LBO limit of various syngas mixtures at a moderate swirl number at the same power output using three types of outlet nozzles.

Increasing the mole fraction of the H_2 from 25% to 45% extended the LBO limit of a given fuel mixture by decreasing the LBO equivalence ratio significantly. There is a small effect of the nozzle angle on the LBO equivalence ratio at low flow rates using all mixtures. However, there is a pronounced effect at higher flowrates and blends with low hydrogen content, thus lower Da number. This is believed to be a reflection of the interaction between structures such as the CRV and PVC, that under these lower reacting conditions impact on the flame by increasing stretch that can no longer cope with the phenomenon of blowoff. The use of confinement altered both the size and shape of CRZ, as expected. However, the usage of different blends has also affected considerably the size of the structure, impacting on the turbulence intensity and stretch across the boundaries of this region.

Acknowledgement

The authors gratefully acknowledge the support of the Welsh Government Low Carbon Research Institute Programme, the EPSRC (grant no EP/G060053). Mr. Hesham Baej gratefully acknowledges the support of the Libyan Embassy and the Libyan Cultural and Education Bureau in London.

References

- [1] Megan Karalus, 2013. An Investigation of Lean Blowout of Gaseous Fuel Alternatives to Natural Gas, PhD Thesis, University of Washington.
- [2] Syred N, 2006. A review of oscillation mechanisms and the role of the PVC in swirl combustion systems, *Prog Energy Combust Sci* 32 (2): 93-161.
- [3] Lefebvre A, 1999. *Gas Turbine Combustion*. Second Edition, U.S.A., pp. 400.
- [4] Valera-Medina A, Syred N, Bowen P, 2013. Central Recirculation Zone Analysis using a Confined Swirl Burner for Terrestrial Energy. *J AIAA Propulsion Power* 29(1): 195-204.
- [5] Lieuwen T, 2012. *Unsteady Combustor Physics*, Cambridge Press, U.S.A., pp. 430.
- [6] Longwell JP, Frost EE, Weiss MA (1953). Flame stability in bluff body recirculation zones. *Indust Eng Chem* 8: 1629-1633.
- [7] Shanbhogue SJ, Husain S, Lieuwen T, 2009. Lean blowoff of bluff body stabilized flames: Scaling and dynamics, *Prog Energy Combust Sci*, 35: 98-120
- [8] Driscoll J, 2008. Turbulent premixed combustion: flamelet structure and its effect on turbulent burning velocities, *Prog Energy Combust Sci* 34 (1): 91-134.
- [9] N. Peters. *Turbulent combustion*. Cambridge University Press, 2000. ISBN 007-1169105.

- [10] Lieuwen, T.; McDonell, V.; Petersen, E.; Santavicca, D. Fuel flexibility influences on premixed combustor blowout, flashback, autoignition, and stability. *J. Eng. Gas Turbines Power* 2008, 130, 011506.
- [11] Lee, M. C.; Seo S B; Yoon J; Kim M; Yoon Y. (2012). "Experimental study on the effect of N₂, CO₂, and steam dilution on the combustion performance of H₂ and CO synthetic gas in an industrial gas turbine." *Fuel* 102(0): 431-438
- [12] Strakey, P; Sidwell, T; Ontko, J (2007). "Investigation of the effects of hydrogen addition on lean extinction in a swirl stabilized combustor." *Proceedings of the Combustion Institute* 31(2): 3173-3180.
- [13] Schafer, R. W., Wicksall, D.M; Agrawal, A.K (2002). "Combustion of hydrogen-enriched methane in a lean premixed swirl-stabilized burner." *Proceedings of the Combustion Institute* 29(1): 843-851.
- [14] Zimont, V., Polifke, W., Bettelini, M., and Weisenstein, W., July, "An Efficient Computational Model for Premixed Turbulent Combustion at High Reynolds Numbers Based on a Turbulent Flame Speed Closure," *J. of Gas Turbines Power*, 120, 526- 532(1998). 16(C): 288-296.
- [15] Date A W, 2005. *Introduction to Computational Fluid Dynamics*, Cambridge University Press
- [16] Poinso T, Veynante D, 2005. *Theoretical and Numerical Combustion*, R.T. Edwards, U.S.A., pp. 522.
- [17] Versteeg HK and Malalasekera W, 1995, *An Introduction to Computational Fluid Dynamics – The Finite Volume Method*, Longman Group Ltd.
- [18] Zimont V, 2000. Gas Premixed Combustion at High Turbulence. *Turbulent Flame Closure Model Combustion Model. Exp Thermal Fluid Sci* 21:179– 186.
- [19] Hesham Baej et al. Impacts on blowoff by a variety of CRZs using various gases for gas turbines *Energy Procedia* 61 (2014) 1606 – 1609.
- [20] Viguera-Zuniga MO, Valera-Medina 2012. Studies of the precessing vortex core in swirling flows. *Journal of Applied Research and Technology* 10 (5) , pp. 755-765.
- [21] Viguera-Zuniga MO, Valera-Medina A, Syred N, Bowen P. High Momentum Flow Region and Central Recirculation Zone